

# Solar Energy Inputs Estimation for Urban Scales Applications

Luis Merino<sup>1</sup>, Eduard Antaluca<sup>1</sup>, Bulent Akinoglu<sup>2</sup>, Benoit Beckers<sup>1</sup>

(<sup>1</sup>) Avenues – Urban Systems Engineering Department  
Compiègne University of Technology, FRANCE

(<sup>2</sup>) Middle East Technical University, Ankara, TURKEY

## 1. ABSTRACT

Solar gains, air and heat exchange, internal gains and auxiliary energy sources are key aspects when dealing with building and urban energy balances. This work tackles the first issue, by using a simple model based in a work made in 1960 to calculate solar radiation components in clear days: direct and diffuse. The main goal is to clarify the differences between the calculations of this early model and the real measurements of the two components of solar irradiation to use in the urban context. The methodology is simple and the results give some rough conclusions about the differences in the measured and calculated values to be use for energy balance calculations. This work is a preliminary study of the adjustment of the method of calculations used in the software Heliodon 2. The model was tested using 10 years data of solar radiation from USA.

**Keywords:** solar radiation, theoretical and measured values, sky view factor, statistical analysis.

## 2. INTRODUCTION

Solar radiation and its components have been estimated by several methods and models (Duffie and Beckman, 2006) during the past years and, the number of models for estimating the solar radiation is considerable. Hence the dilemma we face: to choose and to use a good model for predicting the solar radiation and at the same time to use the minimum data for its calibration. This is a difficulty due to the lack of worldwide available data. Therefore, it is convenient to use a simple model formulation that requires low data input for its calibration. Besides, the data must be generic enough to find them anywhere.

In practical applications, the most common situation is to have a tilted surface and needs to calculate the incoming radiation on it. In this case, the total solar radiation is the sum of direct, diffuse and reflected radiation components. When surfaces are surrounded by other structures that mask part of the sun path (urban context), the solar radiation components are difficult to calculate because of various aspects like shadow, geometry, portion of the sky from which the sunlight is obstructed by structures (shading mask) and reflection/absorption properties of surfaces surrounding the surface in study. Moreover, we must include in the analysis of this problem the statistical distribution of the daily total radiation due to various categories of days of differing degrees of cloudiness.

Solar irradiation reaching the earth is a fraction of the extraterrestrial solar irradiation wich is related to the solar constant. Liu and Jordan (1960) calculated these fractions on a horizontal surface at ground level. In this study, they calculated these factors for the direct radiation (ratio of intensity of direct radiation at normal incidence that reaches the ground surface and intensity of solar radiation at normal incidence outside the atmosphere of the earth), diffuse radiation (ratio of intensity of diffuse radiation on a horizontal surface and intensity of solar radiation incidence upon a horizontal surface outside the atmosphere of the earth) and total

radiation. These ratios are called atmospheric transmittance and were calculated from measurements made at Hump Mountain (Moore and Abbot, 1929), Blue Hill (Hand, 1954) and Minneapolis (Liu and Jordan, 1960). The extreme values of the atmospheric transmittance are shown in Table 1. The authors found a good level of agreement between the regression obtained from Hump Mountain and the values of the other two locations.

*Table 1: Values of direct transmittance.*

<b>Location</b>	<b>Hump Mountain, North Carolina</b>	<b>Minneapolis, Minnesota</b>	<b>Blue Hill, Massachusetts</b>
Altitude above sea level	1463 m	272 m	192 m
Highest Values	0.743	0.706	0.745
Lowest Values	0.425	0.450	0.6 -0.72

The statistical dispersion of these values for clear days was concentrated between 0.6 and 0.7. This indicates that direct atmospheric transmittance ( $\tau_D$ ) values of 0,6 or 0,7 are very realistic for clear-day scenarios. Besides, Liu and Jordan found the following equation for calculating the diffuse transmittance ( $\tau_d$ ) under cloudless conditions by using data from Hump Mountain:

$$\tau_d = 0.2710 - 0.2939 \tau_D . \quad (1)$$

This equation (1) was validated by using data from both the other locations with a good level of accuracy and the authors suggested that this equation is of general validity and should be applicable in broadly where the conditions are similar.

In the present work, we have chosen a simple model based in the idea proposed by Liu and Jordan (1960) by virtue of software Heliodon 2. This model assumes that the solar radiation is a function of the distance the solar beam travels through the atmosphere which is considered by the transmittance of the atmosphere, the extraterrestrial incident flux density (solar constant) and spatial components related to the coordinates of the surface. To obtain the amount of beam radiation that traverses the earth's atmosphere and is incident at the ground level, we need to know the transmission properties of the atmosphere. As we mentioned above, the atmospheric transmittance ( $\tau$ ) to solar radiation of the atmosphere is the fraction of the radiation incident at the top of the atmosphere or extraterrestrial radiation which reaches the ground surface along the vertical (or zenith) path, which is the shortest path length between outer space and the surface. If the slant path is  $m$  times the zenith path, then the transmittance along the slant path will be  $\tau^m$  (Campbell and Norman, 1998; Gates, 2003; Beckers, 2007). In the next section, we describe briefly the model used in this study.

## 2.1 The Model

The total irradiance requires estimating at least three radiations streams:

- direct irradiance on a surface perpendicular to the beam ( $G_p$ ),
- diffuse sky irradiance ( $G_d$ ) and
- reflected radiation from surroundings ( $G_r$ ).

As a first approximation, we are going to work with the two main components of the flux density ( $G_p$  and  $G_d$ ). In this work we assumed isotropic sky and neither reflection nor emission from the surfaces of the scene. Besides, we must remember that these fluxes are energies expressed per unit time and received on a unit area.

The first stream ( $G_p$ ) or the amount of beam solar radiation that reaches the ground surface along a slant is (Campbell, 1998):

$$G_p = G_{sc} \tau^m, \quad (2)$$

where  $\tau$  is the value of the atmospheric transmittance averaged over all wavelengths,  $G_{sc}$  is the solar constant and  $m$  is the air mass. This latter parameter can be calculated at sea level as:

$$m = \frac{1}{\cos \theta_z}. \quad (3)$$

When working at higher altitudes, the value for air mass should be multiplied by a correction factor because of the reduction in atmospheric pressure by:

$$\frac{P}{P_0} = e^{-\frac{z}{8000}}. \quad (4)$$

A general expression can be obtained for calculating the direct solar radiation on a tilted surface with the following equation:

$$G_{\text{tilted}} = G_p \cos \theta, \quad (5)$$

where  $\theta$  is the angle of incidence on the surface and its cosine definition is:

$$\begin{aligned} \cos \theta = & \sin \delta \sin \phi \cos \beta - \sin \delta \cos \phi \sin \beta \cos \gamma \\ & + \cos \delta \cos \phi \cos \beta \cos \omega + \cos \delta \sin \phi \sin \beta \cos \gamma \cos \omega \\ & + \cos \delta \sin \beta \sin \gamma \sin \omega \end{aligned} \quad (6)$$

As solar radiation penetrates the atmosphere, it is depleted by absorption and scattering. Not all of the scattered radiation is lost, since part of it eventually arrives at the surface of the earth in the form of diffuse radiation. The term, diffuse radiation, is used here in the customary way to denote this short wavelength radiation coming from all parts of the sky. It should be distinguished clearly from the atmospheric thermal radiation which, although also diffuse in nature, is of much longer wavelengths (Liu and Jordan, 1960). Besides, if we assume that the sky is an isotropic hemispherical surface, the diffuse component on a horizontal surface for clear days can be calculated as shown in Campbell and Norman (1998) with the following expression:

$$G_d = 0,3 (1 - \tau^m) G_{sc}. \quad (7)$$

This expression is useful in unobstructed sky scenario (i.e. the surface can capture all the diffuse sky radiation), but does not take into consideration the possible obstruction of the sky. This situation is very common in the urban context and one rough way to consider this aspect is by using the view factor. The view factor (also called form factor) is the proportion of the total power leaving one surface and received by another surface and depends only on the shape and relative location of surfaces in the scene (Sillion and Puech, 1994). In urban areas, where land use and geometry change constantly, we need the view factor to take into consideration these heterogeneity and changes. The sky view factor (SVF) is generally used to

describe urban geometry (Svensson, 2004). The definition of SVF is the ratio of the radiation received (or emitted) by a planar surface to the radiation emitted (or received) by the entire hemispheric environment (Watson and Johnson, 1987) and it is a dimensionless value between zero and one. Figure 1 shows two cases of SVF.

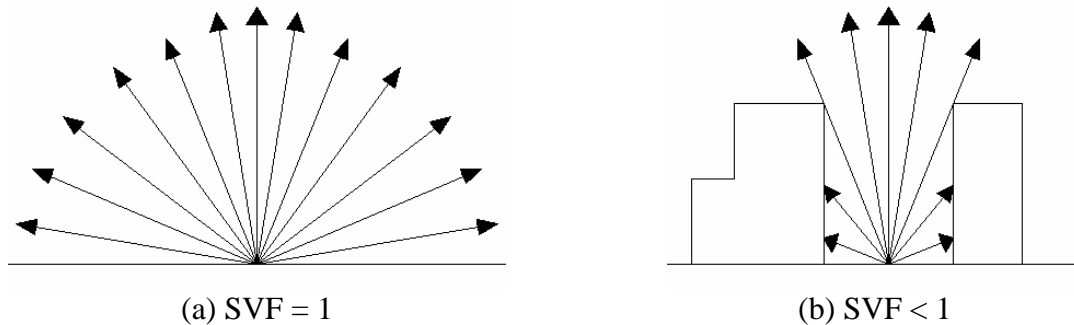


Figure 1: Sky View Factor.

In other words, the SVF is a relationship between the visible area of the sky and the area covered by urban structures. By using the SVF, the total sky diffuse radiation on a horizontal surface could be weighted and this would be a proportion of the theoretical diffuse value. The final expression for the diffuse component in an urban context ( $G_{d-urban}$ ) may approximately be written as:

$$G_{d-urban} = G_d \cdot SVF . \quad (8)$$

The direct and diffuse component expressions were built for clear sky conditions but in practice we have atmospheric effects that affect the intensity of solar radiation because of clouds and other aspects. Due to the extremely variable cloudiness degree, the intensities of direct and diffuse radiation under normal sky conditions will also be highly variable and their values at any one instant are impossible to predict. Therefore, any attempt to establish a relationship for estimating the solar radiation and its components during cloudy days must involve statistical averages which can be obtained from experimental data covering a sufficiently long period of time (Liu and Jordan, 1960).

### 3. DATA AND METHOD

In this section, we will present a short description of the available data which we used to adjust the calculations of the expressions (5) and (7) and also the analysis of the data. As well, a simple preliminary application in the urban context of this methodology will be presented.

#### 3.1 Data

The lack of data on solar radiation records worldwide (Page *et al.*, 2001) is one of the main problems when dealing with solar radiation modeling and forecast in a particular location. Besides, nature of data and level of aggregation is different from place to place. These restrictions are an impediment when trying to obtain a generic model with high global applicability for solar energy evaluation and long-term analysis. An initial effort is made to achieve this purpose, using daily values of solar radiation measurements from the Solar Radiation Monitoring Laboratory of the University of Oregon. The Eugene Station (Latitude: 44,05; Longitude: 123,07; Altitude: 150 m) data was selected for analysing trends and patterns in data. In this case, data aggregation is one day (10-years time-series) and nature of data is global and diffuse radiation on a horizontal surface. The direct component projected

onto a horizontal surface was calculated by subtraction of the diffuse part from the global radiation.

### 3.1.1 Data analysis

A ten-year time-series (1981-1990) has been analysed by covering different periods of aggregation. These periods involve four steps of analysis: daily values, monthly values, seasonal values and finally yearly values. In this work, the term daily values or any other period of aggregation means that this value is total energy captured or integrated over that period per unit area. The seasons were defined as follows: winter begins on winter solstice (December 21), spring on the vernal equinox (March 21), summer on the summer solstice (June 21) and fall on fall equinox (September 21).

The direct and diffuse measured components from time-series mentioned before were analysed graphically and the agreement levels of the expressions (5) and (7) were tested. First, equation (5) was tested by plotting its theoretical values (clear sky conditions) integrated over each day to see differences with daily measurements on a horizontal unitary surface. This was made for each year of the time-series but only the graphs of 1990 are shown due to the similar conclusion obtained. Figure 2 (a) shows a good agreement between the extreme direct measured values and the theoretical clear sky ones. Figure 2 (b) has higher differences but for the degree of agreement here sought the average result is good enough. It should be noted that transmittance value for direct radiation was set to 0.7 (Gates, 2003) and for the diffuse radiation according to equation (1).

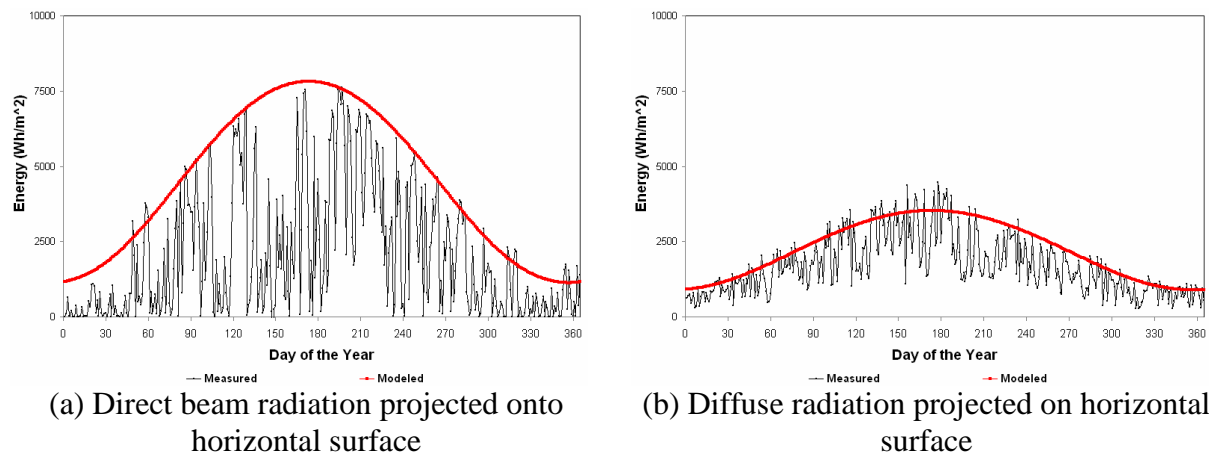


Figure 2: Agreement of theoretical equations with measurements.

In clear days, the calculated values are in good agreement with the measured data. The results shows that the choice of the simple expression (5) with  $\tau_D=0,7$  is a good one. The difuse componet also behaves well as we can seen from Figure 2 (b), although the calculated values are for clear days again, namely equation (7). In principle, the calculations can be adjusted using disagreements with measurements. We use simply the ratios between the measured and calculated values to see the possible deviations within a simple urban street canyon.

In the winter seasons, the measured values of direct radiation are higher than the theoretical ones, this is due to a snow reflection. In warmer seasons, the agreement between these values is quite perfect. Therefore, a general validation of the theoretical expressions was made for extreme cases (clear sky). These expressions must be corrected to take into consideration this effect. The effect of clouds in the solar radiation is evident if we look the Figure 2 (a) and (b),

due to the difference between calculated value and the measured value. We can see that calculated values form an envelope or upper bound of the measured values, because calculations are for clear days.

As mentioned before, it is difficult to forecast instantaneous values of solar radiation. Because of this, we analyse data using different levels of integral time. Figure 3 shows the evolution of the quotient or ratio between real and theoretical values. These ratios involved the total energy in each period of study (i.e.: in summer, we calculate the ratio between the total measured energy in that season and the total estimated clear day energy in that season with the equation (5)). Due to the high variability of daily values, we only calculate the ratios by using three integration periods: month, season and year.

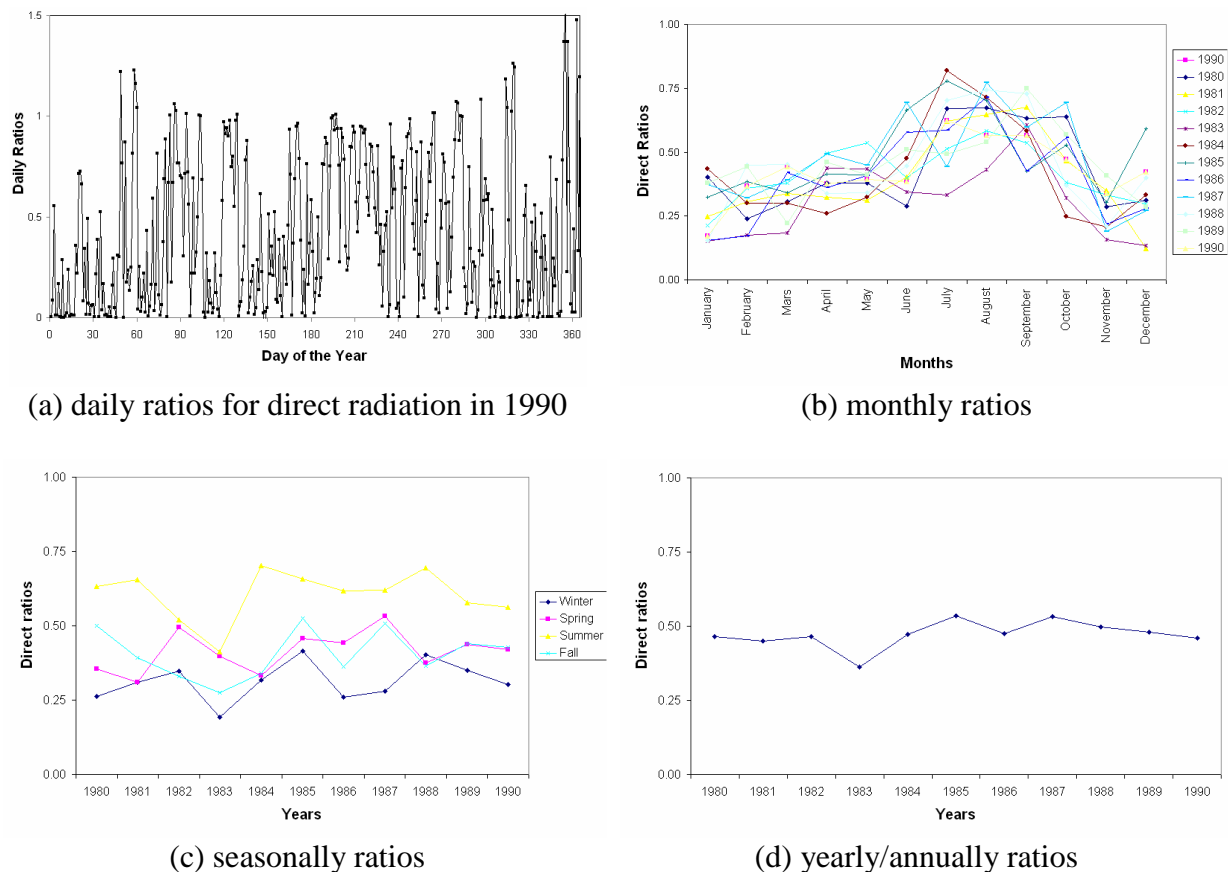


Figure 3: Trends in direct radiation measurements over the time period 1980-1990.

First, in Figure 3 (a) theoretical daily values are compared with the measured values in the 1990. Figure 3 (b) shows the graphical comparison between monthly ratios in each month for the time-series. Figure 3 (c) shows the seasonally ratios in each year of the time-series. Finally, in Figure 3 (d), the ratios in each year are presented. It is clear that variability in ratios decreases according with the length of integration time as expected.

In 1983, the Eugene data were affected by the aerosols from the eruption of El Chichón in Mexico (Vignola and McDaniels, 1985). Because of this specific situation, 1983 is considered an outlier value (i.e.: this observation is numerically distant from the rest of the data). This year is not considered in the data analysis and the year 1980 is added to the time-series. This anomaly is clearer in Figure 3 (d).

One of the most important observations in these four graphs presented above is that the range (difference between the highest and the lowest values) decreases, achieving its minimum by using yearly values. The following tables give the statistics for each level of integration time and their evolution. Table 2 shows statistical analysis of monthly ratios for the direct radiation. Here, averaged ratios increase in summer or warmer months which implies that agreement between calculated and measured values is higher in these months. Variability in ranges also increases in these months.

*Table 2: Statistical analysis of monthly ratios of direct radiation.*

<b>Month</b>	<b>Minimum</b>	<b>Mean</b>	<b>Maximum</b>	<b>Range</b>	<b>Std. Deviation</b>
<b>January</b>	0.15	0.29	0.44	0.28	0.11
<b>February</b>	0.17	0.33	0.45	0.28	0.09
<b>Mars</b>	0.22	0.36	0.45	0.23	0.07
<b>April</b>	0.26	0.39	0.49	0.23	0.08
<b>May</b>	0.31	0.40	0.54	0.23	0.07
<b>June</b>	0.29	0.48	0.69	0.41	0.13
<b>July</b>	0.44	0.63	0.82	0.37	0.12
<b>August</b>	0.54	0.67	0.77	0.24	0.08
<b>September</b>	0.43	0.59	0.75	0.32	0.11
<b>October</b>	0.25	0.49	0.69	0.45	0.13
<b>November</b>	0.19	0.28	0.41	0.22	0.07
<b>December</b>	0.12	0.33	0.59	0.47	0.12

*Table 3: Statistical analysis of seasonal ratios of direct radiation.*

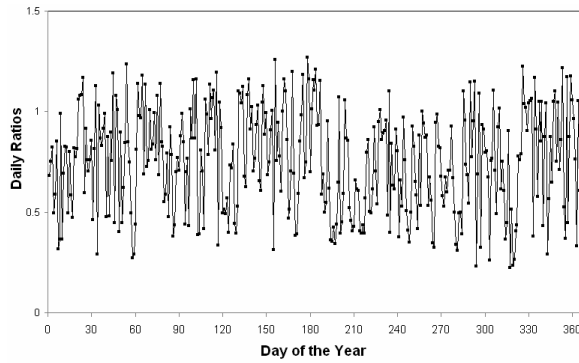
<b>Season</b>	<b>Minimum</b>	<b>Mean</b>	<b>Maximum</b>	<b>Range</b>	<b>Std. Deviation</b>
<b>Winter</b>	0.26	0.32	0.42	0.16	0.05
<b>Spring</b>	0.31	0.42	0.53	0.22	0.07
<b>Summer</b>	0.52	0.62	0.70	0.18	0.06
<b>Fall</b>	0.33	0.42	0.52	0.19	0.07

*Table 4: Statistical analysis of annually ratios of direct radiation.*

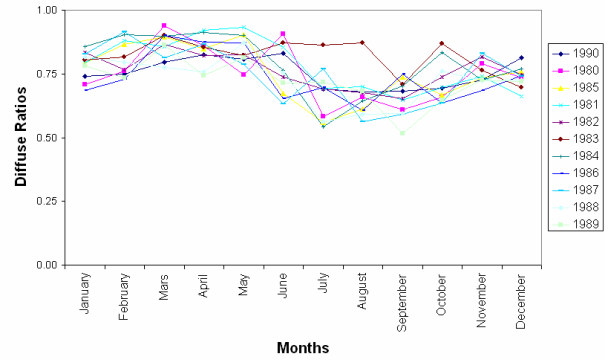
<b>Year</b>	<b>Minimum</b>	<b>Mean</b>	<b>Maximum</b>	<b>Rang e</b>	<b>Std. Deviation</b>
<b>Time-series</b>	0.45	0.48	0.54	0.09	0.03

Tables 3 and 4 show that variability decreases and becomes more stable as the time interval increases. They also show a symmetric variation with respect to the average. As a general trend, the ratio variations tend to decrease with time length aggregation. This behavior is expected, and concurs with experience. The last result is important, because of the lowest variation in annual ratios, reaching less than 10%. It is sensible to say that the direct component has less than 5% of variation with respect to the mean value.

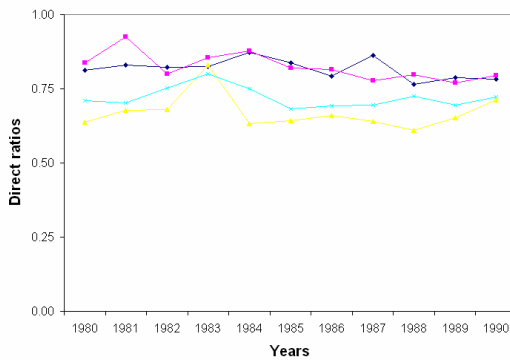
Figure 4 shows the same analysis for the diffuse component and the conclusions obtained are analogous to the direct component case. But the variability of ratios are lower than in the case of direct component. Here, ratios are higher, reaching values over 80% in cold seasons. This is consistent with the graph showed in Figure 4 (a), where we can see clearly that the diffuse component becomes more stable in the extreme cases.



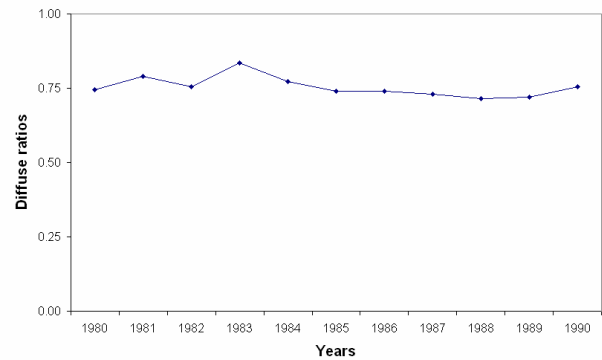
(a) daily ratios for diffuse radiation in 1990



(b) monthly



(c) seasonally



(d) yearly/annually

Figure 4: Trends in diffuse radiation measurements over the time period 1980-1990.

Table 5 and 6 present the ratios and some statistical information for the diffuse component of solar irradiation.

Table 5: Statistical analysis of seasonal ratios of diffuse radiation.

Season	Minimum	Mean	Maximum	Range	Std. Deviation
Winter	0.77	0.82	0.87	0.11	0.03
Spring	0.77	0.82	0.92	0.16	0.05
Summer	0.61	0.65	0.71	0.10	0.03
Fall	0.68	0.71	0.75	0.07	0.02

Table 6: Statistical analysis of annually ratios of diffuse radiation.

Year	Minimum	Mean	Maximum	Range	Std. Deviation
Time-series	0.72	0.75	0.79	0.07	0.02

Finally, we present in Tables 7 and 8, the statistical analysis for the global radiation on a horizontal plane. In this case, the ratios in each period of time integration are almost constant, around 55%.

Table 7: Statistical analysis of seasonal ratios of global radiation.

Season	Minimum	Mean	Maximum	Range	Std. Deviation
Winter	0.46	0.51	0.57	0.11	0.03
Spring	0.50	0.54	0.61	0.11	0.04
Summer	0.57	0.63	0.68	0.11	0.03
Fall	0.49	0.53	0.58	0.10	0.04

Table 8: Statistical analysis of annually ratios of global radiation.

Year	Minimum	Mean	Maximum	Range	Std. Deviation
Time-series	0.56	0.57	0.60	0.05	0.02

Tables 4, 6 and 8 show that yearly ratios are quite stable. Therefore, we could say that with a goof level of accuracy that direct, diffuse and global energy in one year are 48%, 75% and 57% of the calculated value, respectively. In conclusion, we can say that the ratios of calculated yearly integrated clear day values to that of measured are quite stable for different years. In addition, seasonal time intervals may be also considered to give stable ratios. For this reason, we can use the average ratios to adjust the theoretical clear sky values.

### 3.2 Application and Methodology: Urban Canyon

As we mentioned before, the values of direct and diffuse components could be estimated easily with the expressions (5) and (7). The energy is the numerical integration of these instantaneous values obtained with these two expressions and the total theoretical radiation on the surface will be the sum between the integrated values of direct and diffuse components. Finally, we will obtain a theoretical quantification of the energy that could be corrected with the average ratios presented in the previous section. This methodology is explained in more details using a simple simulation. Here, we use a typical simple urban case in which the horizontal surface of interest has sun obstructions. These obstructions are produced by a straight semi-infinite corridor (urban canyon) as shown on Figure 5.

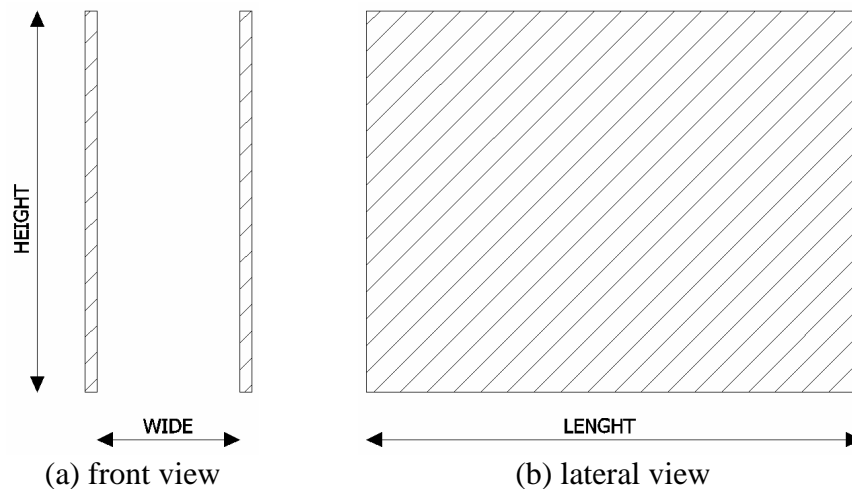


Figure 5: semi-infinite corridor.

In this urban case, a horizontal square surface of  $1 \text{ m}^2$  is located at ground level with its centre in the middle of the canyon. The orientation of the canyon is North-South and we will considerer black walls to neglect reflections on the surface. Another assumption is that there is no radiative exchange between surfaces. The adopted values of height and wide are 16 m and 7 m respectively. The length of the corridor is infinite to avoid border effects that could distorsionate the analysis. Five vertical positions of the horizontal surface in the canyon were considered. This provides important information of the real behaviour of each component and global radiation because of variation in SVF. The Figure 6 shows three vertical positions for the horizontal surface and its variation of SVF. The extreme values of SVF are obtained at ground level and at the top of the canyon.

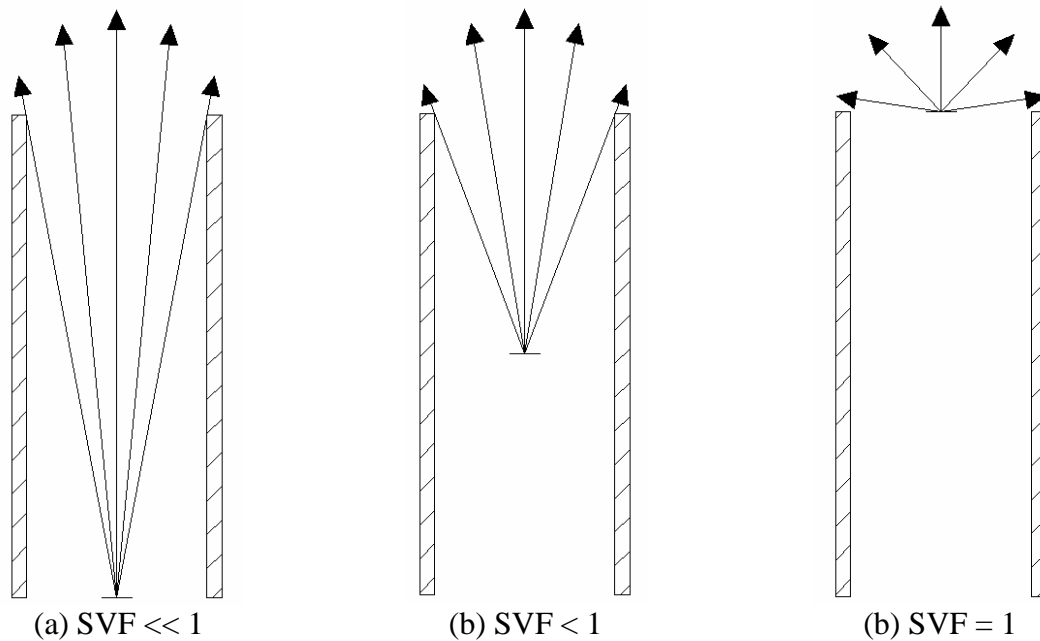


Figure 6: Variation of SVF with height.

The solar radiation components related with each SVF are also shown in Table 9 and Table 10. In these tables, it is clear that SVF increases with height and its maximum value (100%), as we expected, occurs at the top of the canyon. The amount of direct and diffuse energy ( $\text{kWh/m}^2$ ) increases with increasing SVF. SVF values were obtained using the software Heliodon 2. Table 9 and 10 show these SVF values in percentage at different points within the canyon.

Table 9: Theoretical values of direct radiation.

Direct Radiation						
Height	SVF	Winter	Spring	Summer	Fall	Annually
0	22	31	109	111	32	284
4	28	35	142	144	37	358
8	40	55	207	210	57	531
12	66	98	355	359	103	915
16	100	166	542	549	173	1430

Table 10: Theoretical values of diffuse radiation.

Diffuse Radiation						
Height	SVF	Winter	Spring	Summer	Fall	Annually
0	22	16	28	28	16	88
4	28	21	36	37	21	115
8	40	30	51	52	30	164
12	66	50	85	86	49	269
16	100	75	129	131	74	409

The software Heliodon 2 allows to calculate direct and diffuse contribution using expressions (5) and (7). For the direct component takes into account sun obstructions and the diffuse one is ponderated with the SVF (Beckers, 2007). These values are then corrected by using the ratios calculated before. We assumed that the solar irradiation will be transferred within the

urban canyon without any considerable change in ratios. In summary, the methodology for calculating the corrected values is:

$$G_{corrected} = G_{theoretical} \cdot Correction\ factor . \quad (9)$$

Figure 7 shows theoretical values obtained with expressions (5) and (7) and corrected values using seasonal factors in each component. The interpretation of the legend in the graph is: “Direct T” or Direct Theoretical and “Direct C” or Direct Corrected.

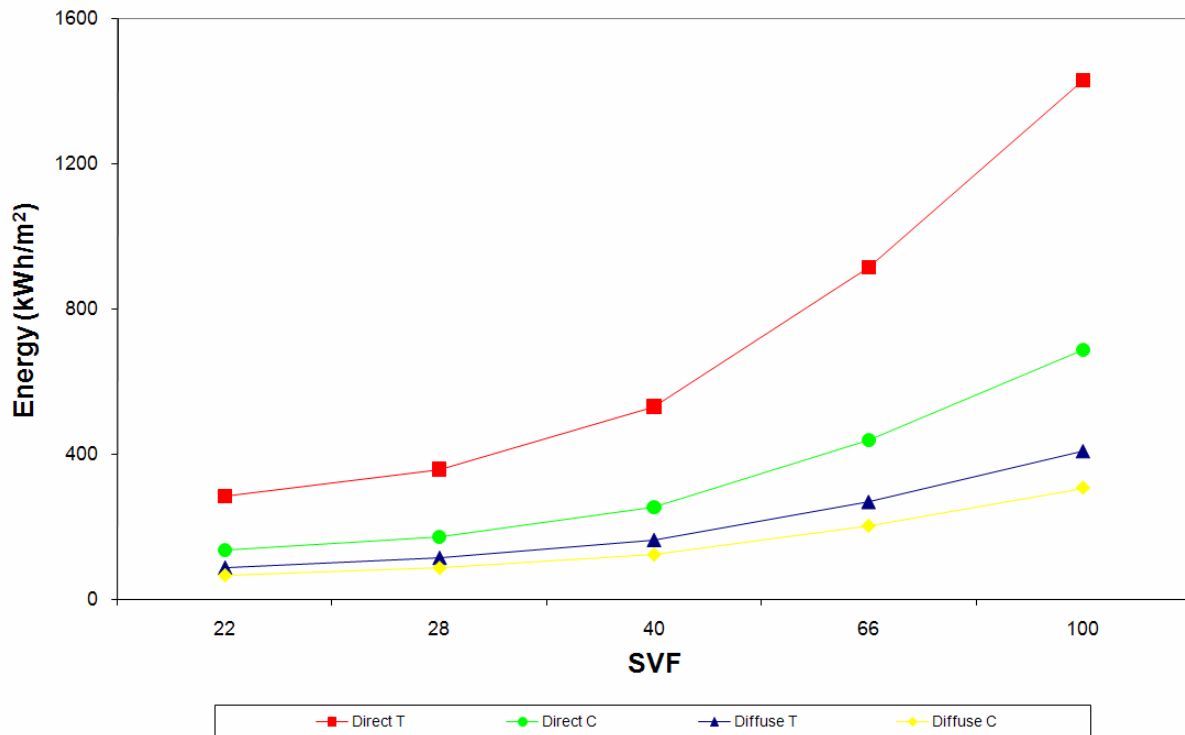


Figure 7: Theoretical and corrected values of direct and diffuse component.

In this graph, we only show corrected values using seasonal ratios because of difference between corrected values using annual or seasonal ratios is marginal. This difference is shown in Table 11. In this table the season column is the weighted sum with ratios of all seasons.

Table 11: Comparison between seasonal and annually corrections in each component.

SVF	Direct Corrections		Diffuse Corrections		Difference (%)	
	Season	Year	Season	Year	Direct	Diffuse
22	138	136	66	66	1.2	0.5
28	176	172	86	86	2.2	0.6
40	259	255	122	123	1.5	1.2
66	446	439	201	202	1.6	0.2
100	694	686	305	307	1.1	0.6

Table 12 shows three forms of correcting theoretical values to obtain the global radiation. First, correcting each component in each season and then adding the components corrected. Second, correcting each component annually and then adding the components. Finally, the

theoretical global radiation is obtained by adding theoretical values of direct and diffuse components and then applying the global factor of 57% shown in Table 8.

*Table 12: Comparison between corrected values.*

SVF	Yearly Theoretical Values			Global Radiation Corrected			Difference (%)
	Direct	Diffuse	Global	Season	Year	Global	
22	284	88	372	204	202	212	4.6
28	358	115	473	261	258	270	4.3
40	531	164	695	380	378	396	4.6
66	915	269	1184	648	641	675	5.0
100	1430	409	1839	999	993	1048	5.3

#### 4 DISCUSSION OF THE RESULTS

The new validation process of the equation (5) and (7) using data from USA gives a good first approximation to the problem. The calculated values are sufficient in analysing extreme conditions (for clear and overcast skies) for designing processes. If we want to reach a deeper analysis, we must take into consideration climatic effects into the model and use measured data from different sites. Calculations replicate reasonable results for theoretical solar radiation components and its variation with SVF.

If we analyse the values of each component, we find that by using seasonal or annual factors we obtain the same result with a small difference, but with seasonal factors we are allowed to analyse smaller scales of time and in some cases to evaluate energy performance in heating or cooling periods of the year. Results show that the different ratios related to the integration time periods lead to the same global result. The best level of stability of the ratios is achieved with yearly values. Seasonal aggregation gives also a good level of certainty.

#### 5 CONCLUSION

The agreement of the expressions (5) and (7) with measured clear day values is good and their use is appropriate. Further validations should be made by using data from other locations.

The ratio with the best level of certainty is when we work with yearly periods of time integration. Then, if we analyse the urban case by using long periods of time, it might be possible to adjust the calculated value with a correction factor obtained statistically from measured data. In case of a long-term analysis, working with annual factors is suggested. It is necessary to conduct a deeper analysis of solar radiation data in other locations to find data trends. This methodology of correction suggests that it might be possible to divide the areas into zones to find standard average ratios for each area.

Working independently with each component facilitates trends analysis of data. In this specific case of a canyon, the results show small differences between seasonal and annually weighted calculated values. According to this, we can say that it might be possible to correct calculated values of global radiation (sum of the direct and diffuse components) by using global radiation records. This would overestimate the global radiation calculations, but could be corrected again to obtain a more accurate value with the small difference found in each case. This is helpful due to a worldwide availability of global radiation records.

Moreover, it is also important to carry out other calculations with several urban scenarios, where the geometry and border conditions are different to the urban canyon analysed. This will give an idea of possible patterns and behaviour in ratios. Future works will pursue to analyse tilted surfaces scenarios. This is a difficulty, due to the lack of that kind of measured data.

## REFERENCES

- Beckers, B. & Masset, L., HELIODON 2, 2003-2010. Software and user's guide, www.heliodon.net.
- Beckers, B., Masset, L. & Beckers, P., 2007, *Una proyección sintética para el diseño arquitectónico con la luz del sol*, 8<sup>th</sup> Ibero-american Conference of Mechanical Engineering CIBIM08, October 23-25, Cusco.
- Campbell, G. and Norman, J., 1998. *An Introduction to Environmental Biophysics*. Springer, New York.
- Cooper, P. I., 1969. The absorption of solar radiation in solar stills. *Solar Energy*. **12**. 3.
- Duffie, J.A. and Beckman, W.A., 2006. *Solar energy of thermal processes*. Wiley, New Jersey.
- Gates, D. M., 2003. *Biophysical Ecology*. 1<sup>st</sup> ed. Dover Publications, Mineola, New York.
- Hand, I. F., 1954. Methods of calculating solar radiation values at Blue Hill Observatory, Milton, Massachusetts. *Monthly Weather Review*. **82**. 43-49.
- Liu, B.Y.H and Jordan, R.C., 1960. The interrelationship and characteristics distribution of direct, diffuse and total solar radiation. *Solar Energy*. **4**(3). 1-19.
- Moore, A. F. and Abbot, L. H., 1920. The brightness of the sky. *Smithsonian Miscellaneous Collection*. **71**(4). 1-36.
- Page, J., Albuissou, M. and Wald, L., 2001. The European solar radiation atlas: a valuable digital tool. *Solar Energy*. **71**. 81-83.
- Sillion, F. X. And Puech, C., 1994. *Radiosity & Global Illumination*. Morgan Kaufmann. San Francisco, CA.
- Svensson, M., 2004. Sky view factor analysis-implications for urban air temperature differences. *Meteorological Applications*. **11**. 201-211.
- Vignola, F. and McDaniels, D. K., 1985. Effects of El Chichón on Global Correlations. *Proceedings of the Ninth Biennial Congress of the International Solar Energy*. Montreal, Canada. June. 2434.
- Watson, I. D. and Johnson, G. T., 1987. Graphical estimation of sky view factors in urban environments. *Journal of Climatology*. **7**. 193-197.

## ACKNOWLEDGEMENTS

PhD. Frank Vignola, Director of the *Solar Radiation Monitoring Laboratory* of the University of Oregon for the help in the use and interpretation of solar data.

## NOMENCLATURE

The following notes are taken from Duffie and Beckman (2006).

$\tau_d$ : diffuse transmittance or transmission coefficient for diffuse radiation on a horizontal surface

$\tau_D$ : direct transmittance or transmission coefficient for direct solar radiation

$P$ : pressure at the altitude  $z$ .

$P_0$ : pressure at sea level.

$z$ : altitude in meter above sea level.

$G_{sc}$ : solar constant is the rate at which solar energy is impinging upon a unit surface, normal to sun's rays, in free space, at the earth's mean distance from the sun. In other words,  $G_{sc}$  is the energy from the sun per unit time received on a unit area of surface perpendicular to the direction of propagation of the radiation at mean earth-sun distance outside the atmosphere and its units in the International System of units is  $W/m^2$ .

$m$ : air mass is the ratio of the mass of atmosphere through which beam radiation passes to the mass it would be passing through if the sun were at zenith. Thus at sea level  $m=1$  when the sun is at the zenith and  $m=2$  for a zenith angle  $\theta_z$  of  $60^\circ$ .

$\theta_z$ : zenith angle is the angle between the vertical and the line to the sun, that is, the angle of incidence of beam radiation on a horizontal surface.

$\theta$ : angle of incidence is the angle between the beam radiation on a surface and the normal to that surface.

$\phi$ : latitude, is the angular location north (positive) or south of the equator ( $-90^\circ \leq \phi \leq 90^\circ$ ).

$\delta$ : declination, is the angular position of the sun at solar noon (i.e., when the sun is on the local meridian) with respect to the plane of the equator, north positive;  $-23,45 \leq \delta \leq 23,45$ . The declination  $\delta$  can be estimated approximately with equation of Cooper (1969).

$$\delta = 23,45 \sin\left(360 \frac{284 + \text{day of the year}}{365}\right), \quad (10)$$

$\beta$ : slope, is the angle between the plane of the surface in question and the horizontal ( $0^\circ \leq \beta \leq 180^\circ$ ).

$\gamma$ : surface azimuth angle, is the deviation of the projection on a horizontal plane of the normal to the surface from the local meridian, with zero due south and west positive ( $-180^\circ \leq \gamma \leq 180^\circ$ ).